Printability assessment of cement-based materials based on rheology, hydration kinetics, and viscoelastic properties

Ilhame Harbouz, Emmanuel Roziere, Ammar Yahia, Ahmed Loukili

Printability assessment of cement-based materials based on rheology, hydration kinetics, and viscoelastic properties

Ilhame HARBOUZ[1,2], Emmanuel ROZIERE[1], Ammar YAHIA[2], Ahmed LOUKILI[1*]

[1] Institut de recherche en génie civil et mécanique, UMR CNRS 6183, Ecole Centrale de Nantes, 44321, Nantes cedex 3, France

[2] Université de Sherbrooke, Sherbrooke, Québec J1K 2R1, Canada

Highlights:

- Workability, Extrudability, and Buildability (WEB) requirements were linked to material properties.
- Restructuring parameters were suggested to assess the extrudability of cement-based materials.
- The influence of mix-design parameters on WEB aspects was captured.
- Advanced rheology, hydration evolution, and viscoelastic properties combined to predict the printability of cement-based materials.

Abstract

Designing printable cement-based materials aims to achieve targeted properties to fulfill the specific performance criteria. At fresh state, the material should satisfy particular rheological requirements to achieve a tradeoff between its workability (W), extrudability (E), and buildability (B). Given the printability criteria to be fulfilled, the selection of suitable mixture design is of the utmost importance to ensure successful 3D printing process and good structural performance, which is linked to the material's strength and stiffness properties (E, G) of the print elements. In this study, the printability of different mixtures was evaluated. The properties of the investigated mixtures were varied by mean of paste content and superplasticizer dosages (SP), viscosity-modifying admixture (VMA), and supplementary cementitious materials (SCMs). The isothermal calorimetry, static yield stress evolution, strain sweep, restructuration indices, and ultrasonic wave responses of the investigated mixtures were assessed and used to evaluate their printability. Comparison between selected material properties and printing data allowed establishing useful recommendations to select the mixture with targeted properties for successful printing and adequate structural performance.

Keywords: Printable cement-based materials, Workability (W), Extrudability (E), Buildability (B), paste volume, viscosity-modifying admixture (VMA), supplementary cementitious materials (SCMs), rheology, viscoelastic properties, structuration kinetics.

* Corresponding author

1. Introduction

Across the board, the covid-19 pandemic has had far-reaching consequences on the world of work. For the construction field, many unscheduled closures of jobsites, supply chain issues, lack of materials, and projects put on hold occurred in early 2020. These issues have had great impact on productivity, workforce, and stunted cash flow for many businesses [1]. Meanwhile, the construction digitalization grasped great interest due to the advantages that 3D printing has shown in coping with this health crisis [1]. Indeed, the use of 3D printing technology in construction industry can reduce the number of workers construction's sites and ensure continuous project processing with remote control via Building Information Modeling (BIM) tools. Moreover, this technology allows more architectural freedom and enhances construction sustainability by minimizing wastes. Also, it reduces the construction time and costs by operating at a constant rate [2, 3], hence improving productivity. However, there are some drawbacks that should be tackled before considering its use at large scale. The major challenge is to design mixtures with adequate properties for successful 3D printing processing. Various types of construction materials with adapted properties for each 3D printing step have been experimented. However, selecting the required properties for each step is a very complicated task, given the different compromises to be achieved. Printable cement-based materials should be fluid to facilitate extrusion, but stiff enough immediately after printing to ensure good buildability. Thus, mastering and controlling rheological properties at each processing step are required to ensure successful printing. This necessitates tailoring very different and sometimes contrasting rheological requirements depending on the printing step. In order to take into consideration the overall printability aspects, a new WEB approach, reflecting Workability, Extrudability, and Buildability, is suggested in this study to design cement-based materials to be used in the layered extrusion printing process. Unlike the research studies reported in the literature [4–6], where the chosen parameters related to workability and buildability are independent, WEB parameters are chosen in a way to consider the interaction between the three aforementioned aspects. Workability will, therefore, be assessed in terms of the initial static yield stress ($\boldsymbol{\tau_{s0}}$), its evolution rate with time ($\mathbf{A_{thix}}$), as defined by Roussel [7], and the apparent viscosity ($\boldsymbol{\eta_{app}}$). The initial static yield stress is a key parameter for 3D printing process, especially during the extrusion and deposition phases in which the material can undergo deformations and collapse, if the generated shear stress during printing exceeds the shear threshold value at that time [8]. Combining the 3 parameters will allow us to evaluate the workability of the mixture while taking into account the rate of structuration $\mathbf{A_{thix}}$ also providing a useful insight on the buildability aspect, while the apparent viscosity can capture the microstructural changes with time due to flocculation.

During 3D printing process, the cementitious mixture undergoes considerable agitation during extrusion, i.e. before being deposited as layers, hence resulting in internal structural and rheological changes. These changes and their influence on the shape stability of layers must be taken into account [9]. It is therefore essential to control these variations overtime at the various stages of printing process. The influence of extrusion phase, during which the material can undergo significant deformations, depends on the pumping pressure, diameter of the nozzle, and the extrusion device.

The rheological changes of print material, induced during the extrusion phase was never considered while designing printable materials. In this study, the effect of extrusion on the rheological properties of cement-based materials was evaluated by assessing its restructuration after extrusion, which defines its **Extrudability**. The recovery of the apparent viscosity (**R**), restructuration rate of the storage modulus ($\mathbf{G'_r}$), and the rate of re-flocculation ($\mathbf{R_{thix}}$) as defined by Kruger et al. [10] will be evaluated to predict the effect of extrusion of the printable material. Immediately after extrusion, the strength and rigidity of the printable material become paramount. The evolution of the elastic (**E**) and stiffness moduli (**G**) with the hydration kinetics will be investigated and exploited to assess the **Buildability** aspect of the mixtures. On the other hand, the workability period will be estimated by means of $\mathbf{t_0}$ which represents the open time, i.e. time period before the beginning of the acceleration stage of the cement hydration reaction. The possible interconnections between these parameters are illustrated in **Fig. 1**. It is worth mentioning that a given parameter may be representative of several printability aspects at once.

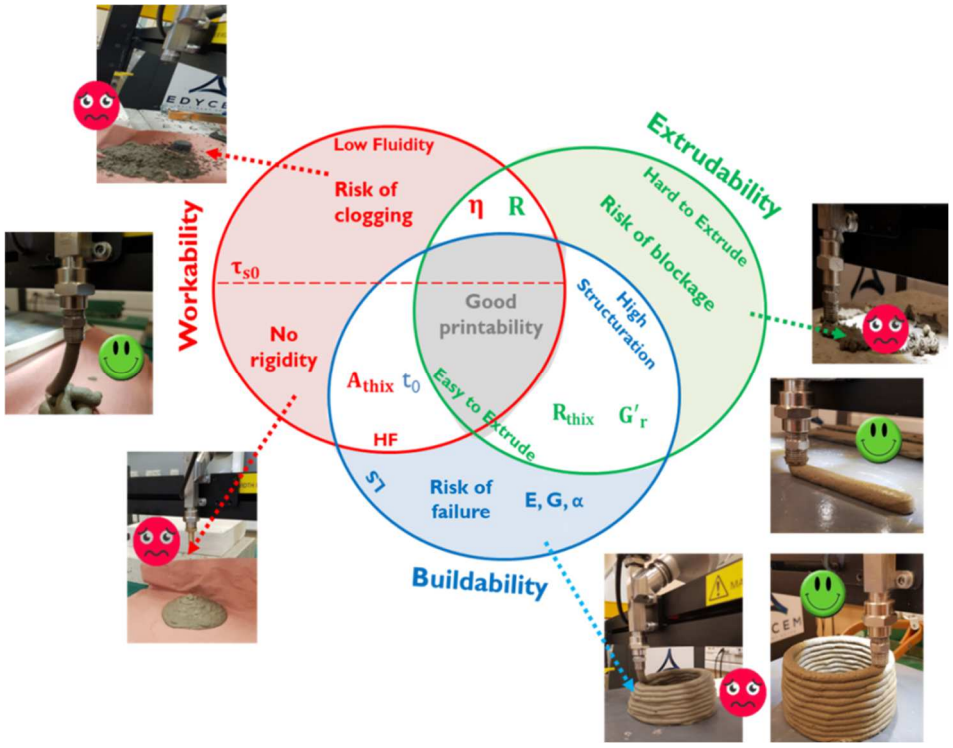

Fig. 1. Key Workability, Extrudability, and Buildability (WEB) parameters

The above-mentioned process requirements can be adapted given the printing process by tailoring proper mixture parameters and design approach to achieve adequate properties. In the present study, different mixture proportioning approaches have been adopted to design cement-based materials for 3D printing. The printability of the investigated mixtures was evaluated according to the WEB concept requirements, as defined earlier. In the first part of this study, the combined effect of paste volume and SP variation on printability aspects was evaluated. Then, two different approaches to improve the printability of mortar were investigated in the second part. In the first approach, the effect of viscosity-modifying admixture (VMA) was analysed. The effect of supplementary-cementitious materials (SCMs) addition was assessed in the second approach. The use of VMA and SCMs aims to cover wide ranges of rheological properties, thus allowing investigating the relevance of different printability criteria.

2. Materials, sample preparation and printing process

2.1 Materials

All the investigated mixtures were portioned using a portland CEM I 52.5 N cement and a compatible polycarboxylate superplasticizer (SP). The chemical compositions and physical properties of CEM I cement are summarized in Table 1. Fontainebleau sand having a specific gravity of 2.65 was used to proportion the mortar mixtures. In general, a maximum ratio of 1/10 is often used between the maximum particle diameter of the sand and the size of the nozzle [9, 10]. However, in order to prevent any risk of blockage, the maximum particle diameter of the sand was limited to 0.4mm. In addition to cement, class F fly ash (FA), silica fume (SF), limestone filler (LF), and kaolinite clay (K) were used. The particle-size distributions of the powder and sand are summarized in Fig. 2. A viscosity modifying admixture (VMA) was used to modify the rheological properties of the mixture and enhance its stability after extrusion [13].

Table 1. Physico-chemical composition of CEM I 52.5 N cement

Chemical analysis (%, by weight)					
CaO	SiO_2	Al_2O_3	Fe_2O_3	SO_3	MgO
63.7	19.6	4.5	2.3	2.6	3.9
Main compounds of clinker (%, by weight)					
C_3S	C_2S	C_3A		C_4AF	
69	9	9		7	
Physical properties					
Normal compressive strength (MPa)		Blaine surface area (cm^2/g)		Density (g/cm^3)	
59		3900		3.13	

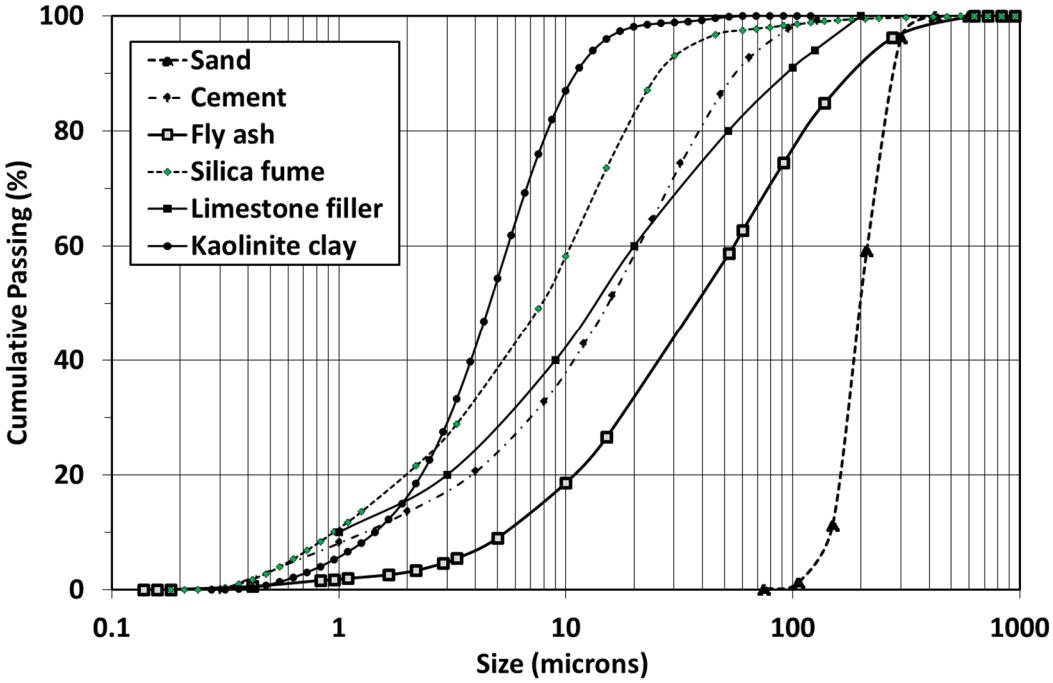

Fig. 2. Particle-size distribution of powders and sand

2.2 Mixture proportions and mixing procedure

The mixture proportions of the mixtures intended for 3D printing are summarized in Table 2. The mixtures were proportioned with a water-to-binder (w/b) ratio of 0.28. First, the combined effect of paste volume and their corresponding SP dosages on printability of mortar mixtures was evaluated. These mortar mixtures are identified by M100, M80, and M63, indicating their paste contents. For example, M100 mixture corresponds to plain paste mixture, i.e. mortar made with 100% of paste. In the second phase of this study, the M63 mortar is then used to evaluate the effect of VMA dosages on its rheological properties. These mixtures are designed by M-x, where x is the dosage of VMA. In addition, three additional mixtures were considered to evaluate the effect of replacing fly ash and silica fume by equal volumes of limestone filler and kaolinite clay. In this part, the M63 mixture will be noted FA-SF for the sake of simplicity. This aims to investigate the effect of SCMs in improving the printability using ternary binders.

The mixtures were prepared using a conventional mortar mixer according to the following protocol. At first, the mixing sequence consisted in introducing dry materials into the mixer and mixing for 1 min at a low speed (140 rpm). Then, the 2/3 of mixing water was slowly introduced while the mixer was rotating. After 1 min of mixing, the remaining mixing water along with admixtures were added and the mixture received another 2 min of mixing. Finally, the edges of the bowl were scraped, and the speed of mixing was increased (285 rpm) for an additional mixing of 2 min, thus allowing a total mixing time of 6 min.

133 Table 2. Mixture proprotions of the investigated mixtures

		Variation of paste volume with SP dosage			Variation of VMA concentration				Effect of LF and K additions		
Mixtures		M100	M80	M63 FA - SF	M-0.2	M-0.5	M-0.8	M-1.5	FA - K	LF - K	LF - SF
Components (kg/m³)	Sand	0	530	981	981	981	981	981	981	981	981
	CEM I	1030	825	650	650	650	650	650	650	650	650
	FA	294	235	185	185	185	185	185	185	-	-
	SF	148	118	93	93	93	93	93	-	-	93
	LF	-	-	-	-	-	-	-	-	200	200
	K	-	-	-	-	-	-	-	93	93	-
	Total binder	1472	1178	928	928	928	928	928	928	943	943
	water	413	330	260	260	260	260	260	260	260	260
Admixtures (%, by weight of cement)	SP	0.3	0.5	1.2	1.2	1.2	1.2	1.2	1.2	1.2	1.2
	VMA	-	-	-	0.2	0.5	0.8	1.5	0	0	0
Water to binder ratio (w/b)		0.28									
Paste volume (l/m³)		100	80	63	63				63		

134 **2.3 Printing process**

135 The printing tests were conducted using a layered extrusion system LUTUM v4.x from *VormVrij*
136 *Company.* This printer is equipped with a 10-mm nozzle diameter functioning under controlled air-
137 pressures and flow rates. First, the mixture was loaded in a cylindrical barrel located above the head
138 of printer. During printing, the pressure generated by compressed air was adjusted given the fluidi-
139 ty of the mixture using a manometer. Extrusion was carried out by means of the worm screw which
140 exerts an additional force on the mixture to push it out of the nozzle. The extrusion device is con-
141 nected to motor and torque limiter to control the extrusion flow rate and the printing speed. These
142 two parameters can be varied from a control box, as shown in Fig. 3. The whole device is mounted
143 on a gantry steering system that allows movement in X, Y, and Z directions (Fig. 3).

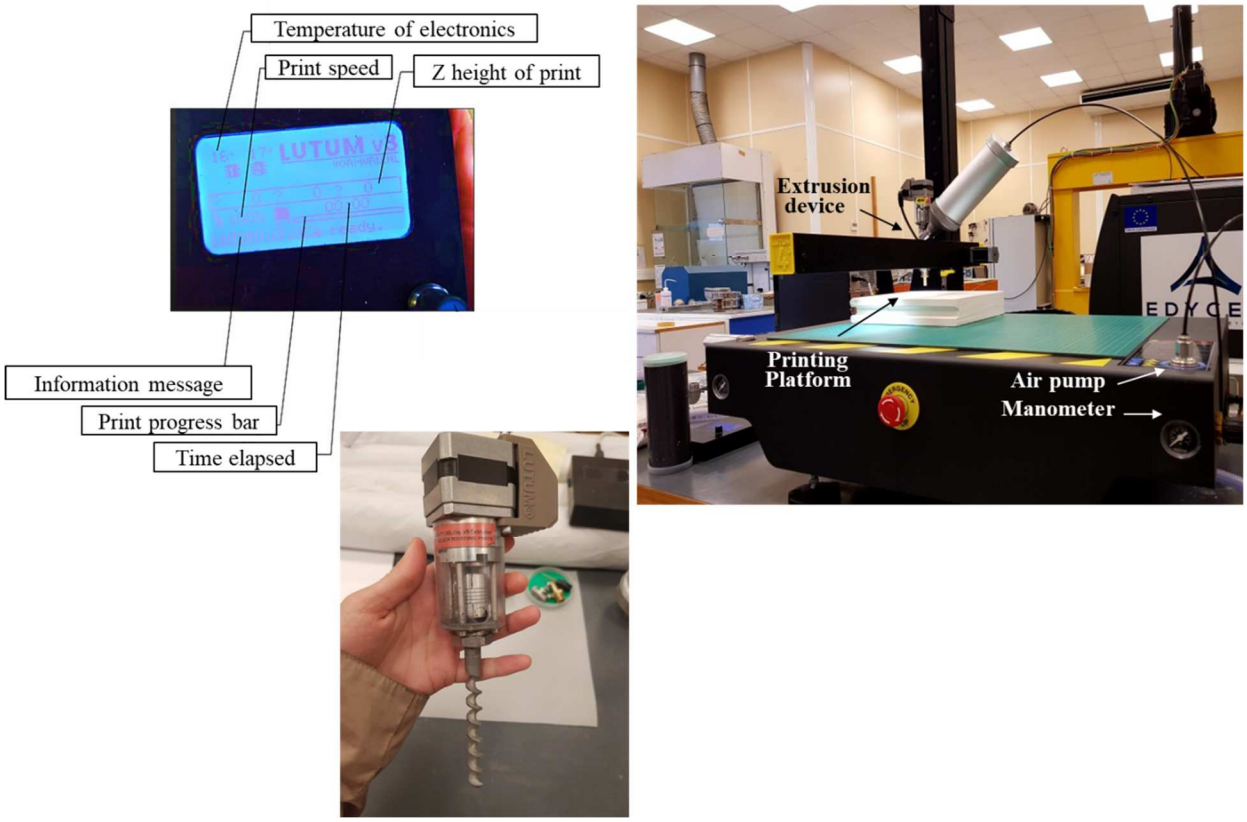

Fig. 3. 3D printer components on the right, control box and the extrusion device on the left

The printability of the investigated mixtures was evaluated by printing circular hollow cylinders. This was evaluated in terms of ease of extrusion and shape stability of the printed cylinders. These aspects were evaluated according to the pumping pressure and number of printed layers. Several series of side-view images of the printed cylinders were captured to compare the textures of different print mixtures. For each mixture, three printing trials were carried out, and an average extrusion pressure and number of printed layers were recorded. The printing parameters are summarized in Table 3.

Table 3. Printing parameters

Printing velocity (mm/s)	Layer height (mm)	Layer thickness (mm)	Pumping pressure (bar)	Flow rate (mm^3/s)
20	5	10	variable	275.71

3. Experimental program

In addition to the rheological properties, the heat of hydration and viscoelastic properties of the printable mixtures were investigated.

3.1 Rheological Measurements

The rheological measurements were performed using Discovery hybrid rheometer from *TA Instruments Company*. The vane-in-cup geometry was used to assess the rheological properties of paste

and mortar mixtures, as shown in Fig. 4. The single-batch method was used for each rheometric test. The diameters of the cup and bob are 30.36 mm and 26.20 mm, respectively, hence providing a shear gap size of 4 mm. The measuring system and tested samples were protected with an enclosure to prevent water evaporation during measurements. On the other hand, all the measurements were performed at a constant temperature of 20°C. Three different rheometry protocols were carried out to assess the static yield stress and its evolution with time, strain sweep, and restructuration tests, as follow.

Fig. 4. The rheometer device and the vane-in-cup used geometry

3.1.1 Static yield stress measurements

The static yield stress of the investigated mixtures was measured by subjecting the sample to a constant shear-rate of 0.01 s^{-1} during 2 min. The peak value of shear stress corresponds to static yield stress, while the shear stress after the thixotropic breakdown corresponds to dynamic yield stress. Initially, the samples were pre-sheared for 2 min using a rotational shear-rate of 200 s^{-1} to achieve a well-defined reference state for all the samples. The sample was then allowed a rest period of 5 min before monitoring the initial static yield stress (τ_{s0}) and thereafter before each measurement (Fig. 5a). The evolution of static yield stress was determined up to 25 min, as shown in Fig. 5b. Since the printing tests were carried out within the first hour after mixing, the subsequent exponential evolution of yield stress reported by Perrot et al. [14] was not assessed in this study. The re-flocculation and linear structuration processes, as well as their corresponding kinetics (R_{thix}, A_{thix}) as defined by Kruger et al. [10] and Roussel [15], respectively, were evaluated. These parameters have been calculated using the equations (1) and (2), as follow:

$$\tau_s(t) = A_{thix}t + \tau_{s,trf} \quad (1)$$

$$\tau_s(t) = R_{thix}t + \tau_{D0} \quad (2)$$

where $\tau_s(t)$ corresponds to static yield stress of the material at time t after the pre-shear (Pa), and τ_{D0} is its initial dynamic yield stress. On the other hand, $\tau_{s,trf}$ corresponds to static yield stress (Pa) of the material after re-flocculation, and is calculated by subtracting from the initial static yield stress τ_{s0}, the structuration that took place during the re-flocculation period ($A_{thix}trf$), as follows: $\tau_{s,trf} = \tau_{s0} - A_{thix}trf$ (**Fig. 6**).

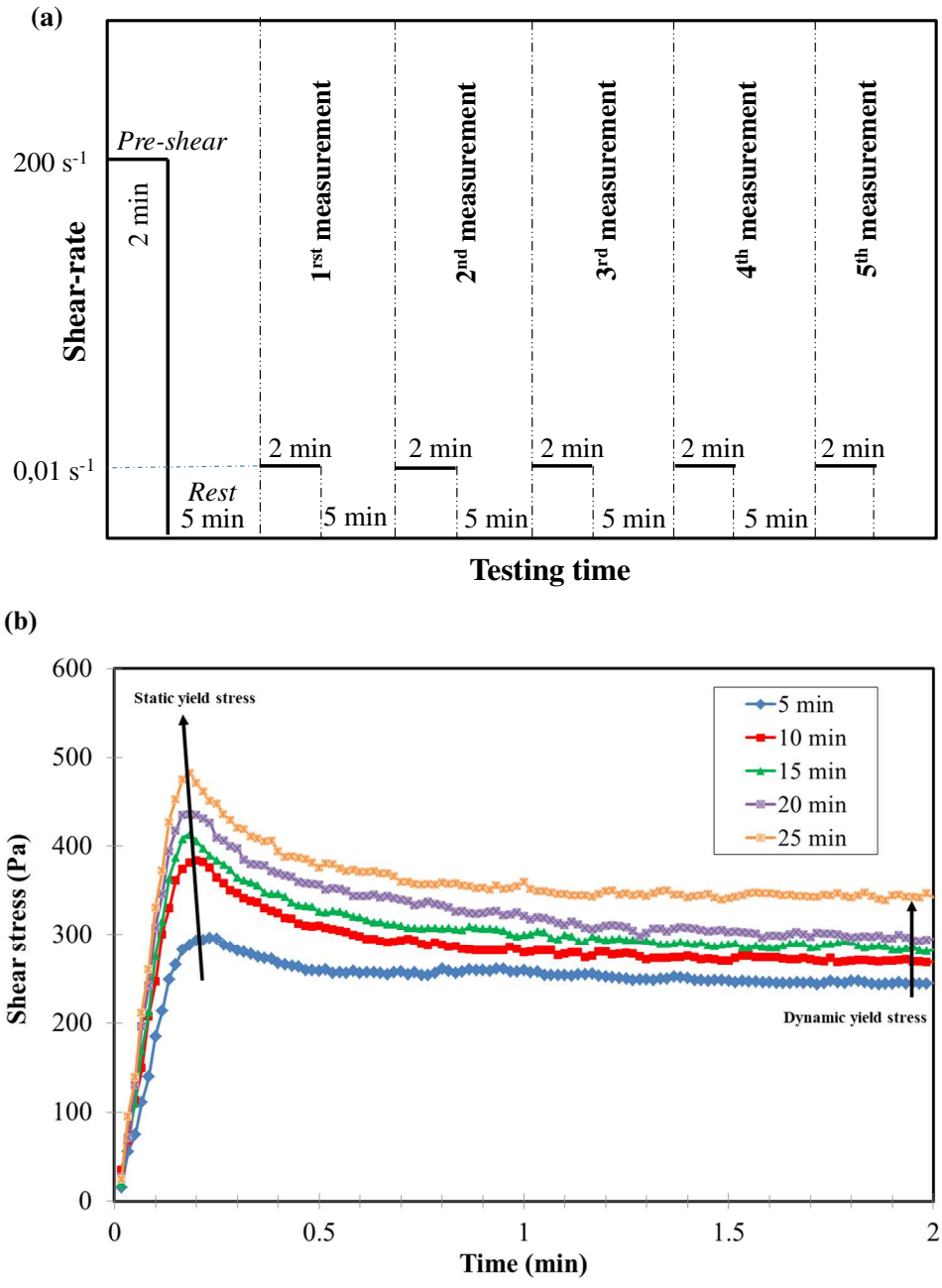

Fig. 5 . (a) Test protocol for yield stress measurement and (b) typical flow onset curve results

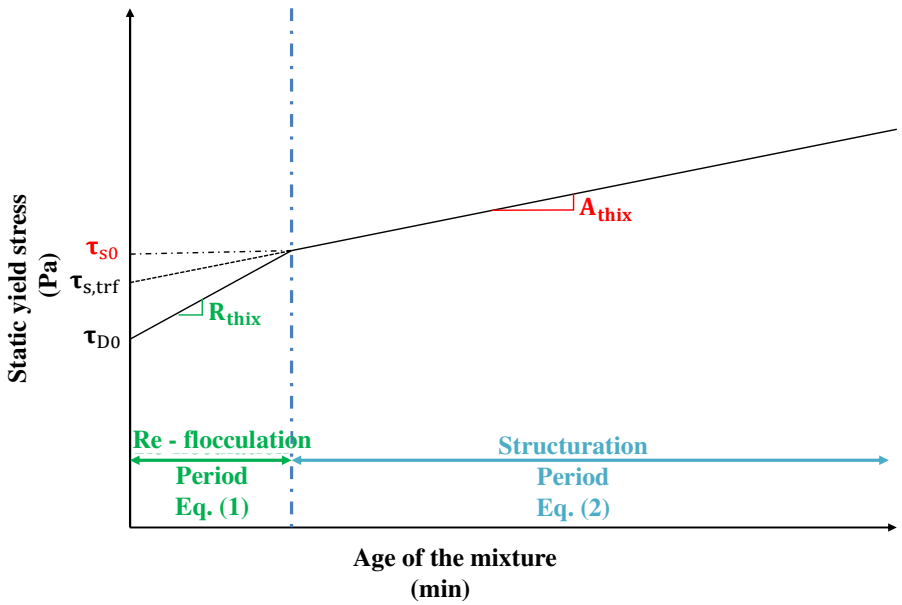

Fig. 6. Evolution of static yield stress with time in both re-flocculation and linear structuration processes [10]

3.1.2 Strain sweep

Strain sweep measurements were performed on printable mixtures to determine their linear viscoelastic regions. This allowed identifying the critical strain to allow carrying out the restructuration tests under undisturbed shear regime. The determination of the critical strain can also provide useful insight into the fresh-state microstructure of the investigated mixtures.

3.1.3 Restructuration kinetics

Two different approaches were used to quantify the restructuration of the investigated mixtures and evaluate the variations of their rheological properties after extrusion (i.e. viscosity and storage modulus), including the restructuration and recovery rates. These approaches are a new way to evaluate the extrudability of cement-based materials. The first approach, known as three-interval thixotropy test (3ITT), consists in first applying a constant frequency within the Linear Viscoelastic Domain (LVD) to identify a well-defined reference state of the sample in non-destructive manner. Afterwards, higher frequency is applied to breakdown the sample microstructure, hence simulating the extrusion process. The final step is similar to the first one in which the reversible restructuration of the sample is assessed. A strain of 0.001% and 10 rad/s frequency were used for the first and third intervals (Fig. 7a). The restructuration parameter (G'_r) represents the slope of the evolution of G' with time.

The second approach consists in assessing the rate of recovery of apparent viscosity after breaking down the structure, as shown in Fig. 7b. First, a very low shear-rate was applied to identify the reference viscosity. A higher shear-rate is then applied to simulate the extrusion process. At the end of shearing regime, the sample was subjected to a low shear-rate of 0.01 s^{-1} to simulate rest condi-

tions, which corresponds to the deposit phase after printing. The recovery apparent viscosity η_1 was then determined and used to calculate the recovery parameter R using Eq. (3), as follow:

$$R = \frac{\eta_1}{\eta_0} \quad (3)$$

where η_1 and η_0 are the initial and recovery apparent viscosities, respectively.

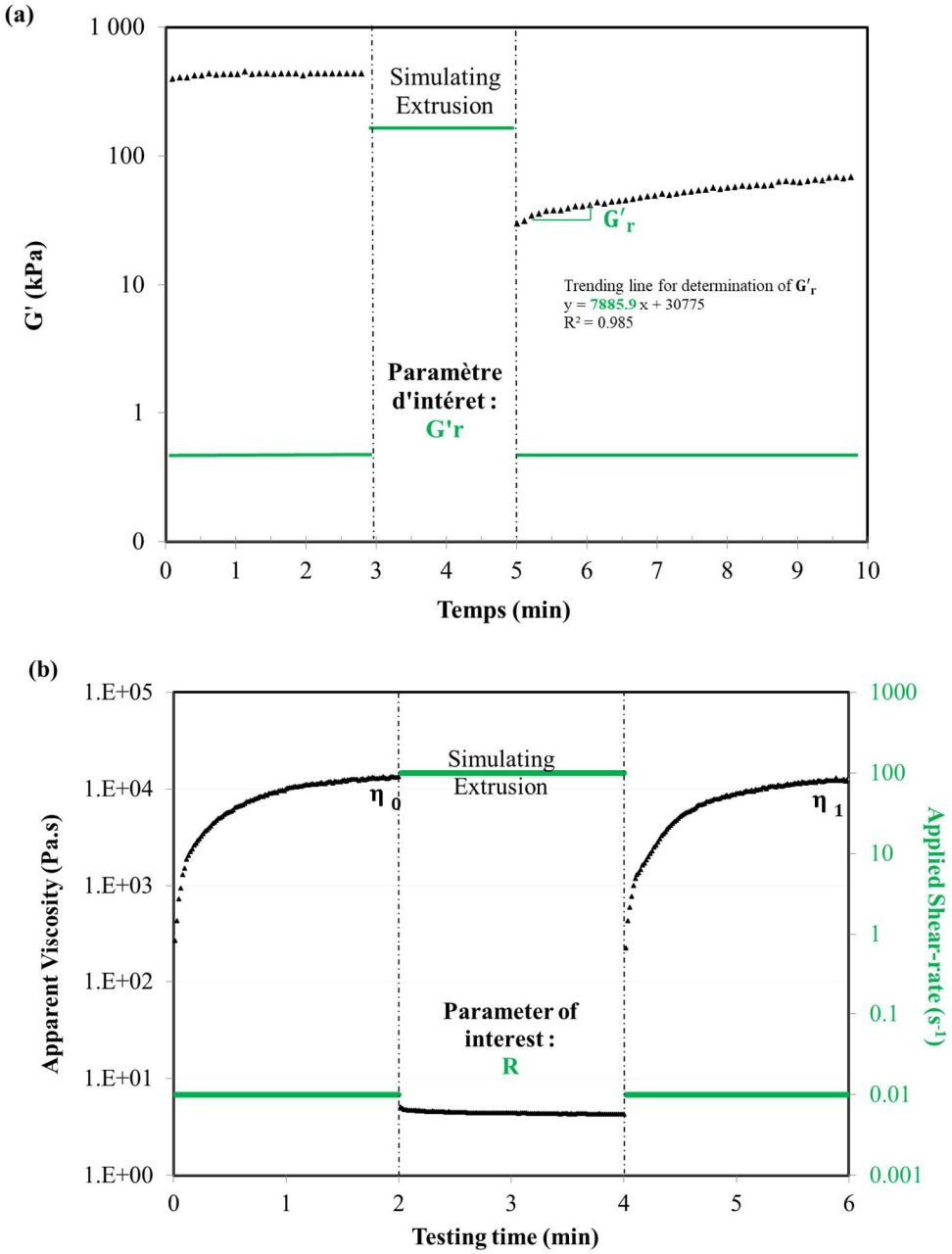

Fig. 7. Protocol of restructuration tests and typical results

3.2 Calorimeter measurements

A TAM Air isothermal micro-calorimeter was used to determine the hydration degree of the investigated mixtures. The measurements were performed using 100-g samples at a controlled temperature of 20°C. The tested samples were prepared using the same mixing procedures described in sec-

tion 2.2, and immediately transferred to the calorimeter. The degree of hydration α was calculated according to Eq. (4), as follow:

$$\alpha = \frac{Q(t)}{Q_\infty} \qquad (4)$$

The workability period was estimated using the open time t_o that represents the induction period (see Fig.8). The influence of mineral additions and VMA dosages on the hydration was evaluated using the mortar M63 as reference mixture. As for the paste content effect, M100 mixture was taken as reference. The normalized t_o is used to investigate the hydration process (delayed if t_o is higher than 1 and accelerated if t_o is lower than 1).

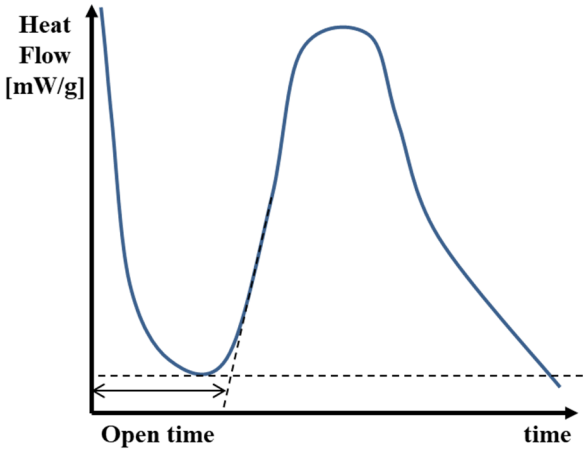

Fig. 8. Determination of the open time t_0 from the isothermal calorimetry measurement

3.3 Elastic properties of the investigated mixtures

The *FreshCon* device was used to monitor the structuration kinetic beyond the setting time of the mixtures. The test was conducted according to the procedures described in the reference [16]. All the measurements were performed in controlled room temperature of 20 ± 2°C. The monitoring of the viscoelastic properties can provide useful information regarding the stiffness and stability of the material after printing. The elastic (**E**) and shear (**G**) moduli were determined from the velocities of compression and shear waves according to Eq. (5) and (6), as follow.

$$E = \left(\frac{3.v_p^2 - 4.v_s^2}{v_p^2 - v_s^2}\right).v_s^2.\rho_c \qquad (5)$$

$$G = v_s^2.\rho_c \qquad (6)$$

4. Results and discussions

4.1 Workability and extrudability parameters

4.1.1 Workability parameters

The workability parameters of the investigated mixtures are summarized in Fig. 9. As can be observed, the reference mixture (i.e. M100) exhibited the highest viscosity, which is due to its low SP dosage, hence resulting in higher colloidal interactions. This accelerated the structuration process, reflected by higher A_{thix} value. In contrast, the M63 mixture containing higher amount of SP exhibited lower viscosity and A_{thix} than M100 mixture, which is due to greater dispersing effect of SP. This is likely to facilitate its pumping but can negatively affect its buildability aspect. On the other hand, the incorporation of VMA significantly increased the viscosity and A_{thix} parameters. This can be mainly due to the long chains and high molecular weight of VMA that absorb the free mixing-water and increase the entanglement effect [17]. It is well established that VMAs modify significantly the rheology of cement-based materials, which to a certain extent increases the macroscopic yield stress [13-16]. There are very few studies in the literature that investigated the effect of VMA on the printability of cementitious materials. Chen et al. [5] evaluated the competitive effects between the dispersive effect of SP and viscous aspect of VMA. This competition can deteriorate the printability of the mixture depending on the resulting balance between the two opposite effects, which is function of admixture dosages and their compatibility. Furthermore, the synergy between the cement, SP, and VMA becomes very critical in this context. The type and chemical composition of cement-SP-VMA system can greatly modify both the fresh and hardened properties of the mixture.

Besides, the type and content of SCMs can significantly change the workability of the mixture. For example, the mixtures containing limestone filler (LF) showed higher fluidity than those incorporating fly ash (FA). Thus, replacing fly ash with limestone filler tends to improve workability of the mixture, reflected by lower viscosity and initial yield stress values. On the other hand, the use of limestone filler induced higher structuration rate. This may be due to the physical effect of limestone filler in modifying the particle-size distribution, packing density, and increasing the heterogeneous nucleation of the system [21]. The higher packing density combined with the low-water demand of LF contribute in improving the fluidity of the mixture, whereas the modification of particle-size distribution and heterogeneous nucleation contribute in increasing A_{thix}.

On the other hand, the replacement of silica fume by kaolinite increased both the initial yield stress and rate of structuration. Due to its high water-demand [22], kaolinite can absorb a significant part of the mixing water, otherwise would normally contribute in lubricating the system and facilitate particles sliding during shear, which decreases the flowability of the mixture. This explains the sig-

nificant increase in viscosity, which is more obvious in the case of FA – K combination than LF – K.

It is worthy to mention that the ranges of workability parameters obtained in this study are comparable with those reported in literature [20–22]. The workability characteristics should be adapted to the printing parameters. For example, stiffer materials can be used for larger scale and different printing processes, as reported in literature [8, 10].

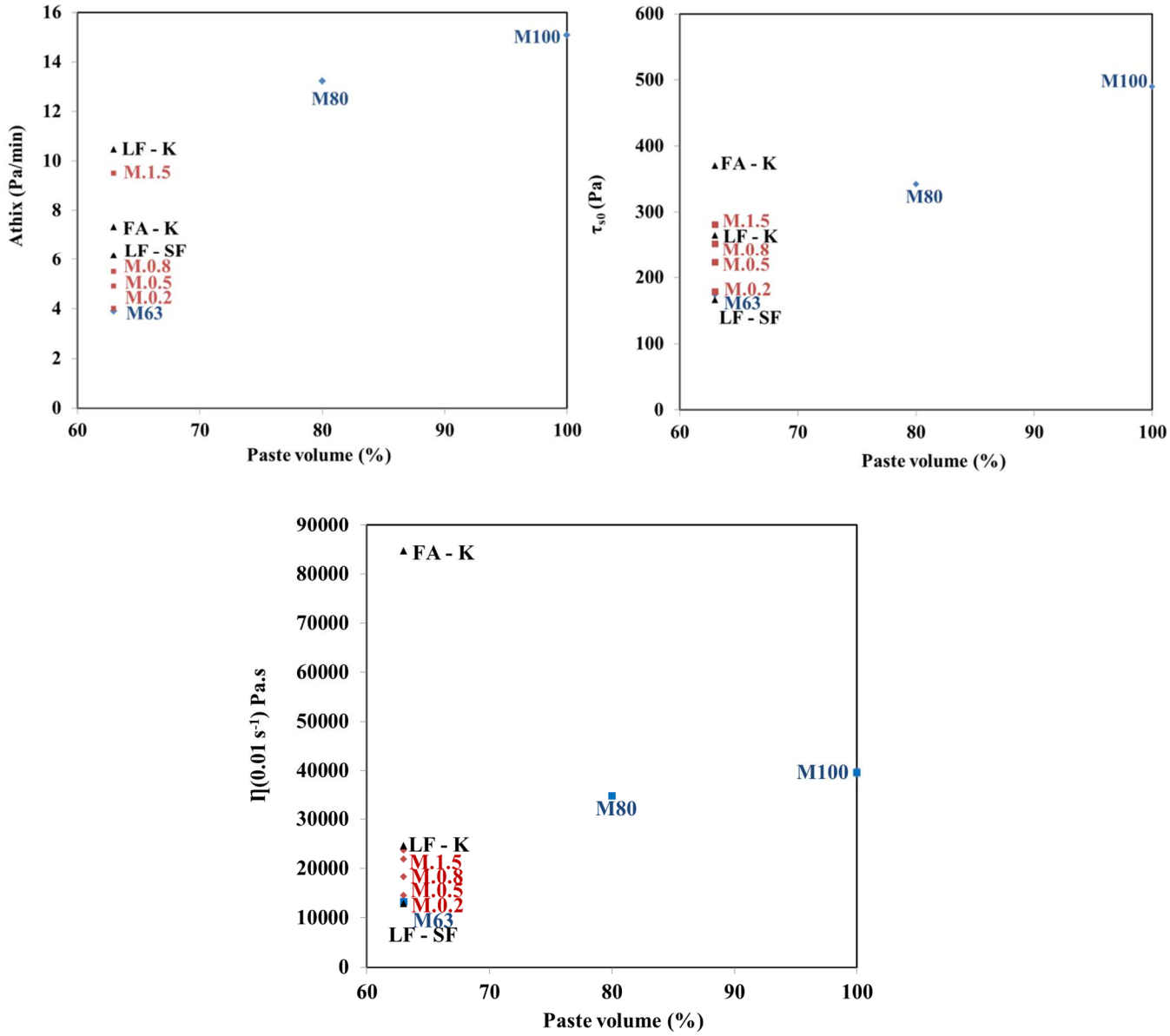

Fig. 9. Workability parameters of the investigated mixtures

4.1.2 Extrudability parameters

Although the previously measured workability parameters provide an insight on the printability of the investigated mixtures, several changes of the material's properties can be expected during pumping and extrusion [26]. As mentioned earlier, a low viscosity is required during the pumping and extrusion processes, but a higher value is needed after extrusion. Eventhough these

requirements appear to be contradictory, they can be easily achieved by exploiting the thixotropy and shear-thinning behaviors of the mixture, as shown in Fig. 10.

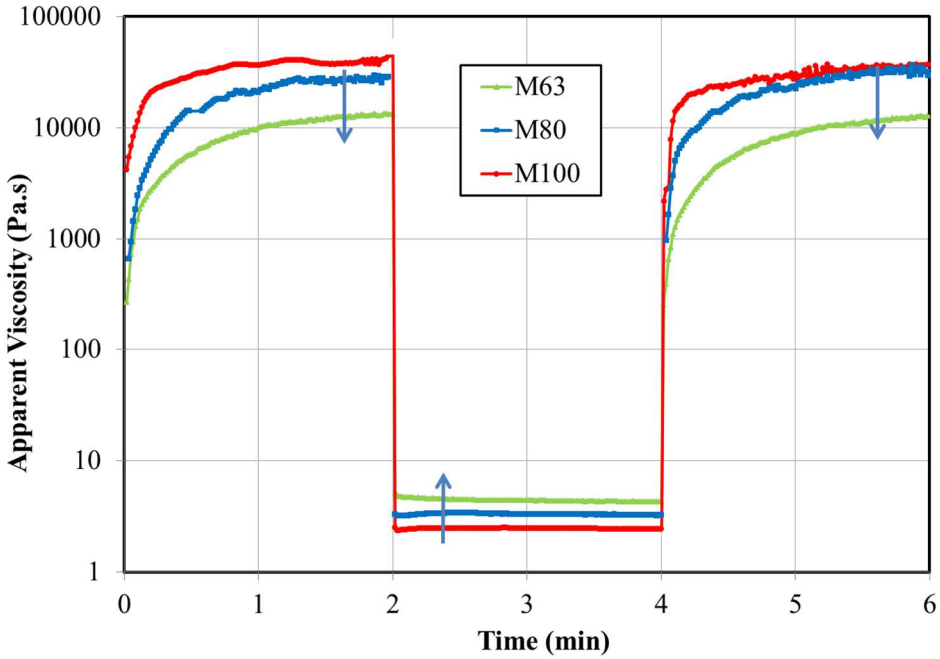

Fig. 10. Variation of apparent viscosity with time during the restructuration tests

The M100 mixture (i.e. no sand) perfectly fulfilled the extrusion requirements, hence justify its common use in the 3D printing applications. This mixture exhibited the lowest apparent viscosity during extrusion, but the highest value at rest.

The extrudability parameters of the investigated mixtures are summarized in Fig. 11. As expected, the M100 mixture showed an increasing recovery rate of R_{thix}, R, and G'_r parameters due to the rapid flocculation of cement particles. The inclusion of sand in cement-based materials inhibits cement particles flocculation, hence reducing the flocculation-induced structuration [27], as reflected by the low R_{thix} value of M63 mixture. This can also be due to the relatively high dosage of SP of the mixture. Indeed, the presence of SP chains induces repulsive interparticle forces and reduce the overall attraction between cement particles and re-flocculation rate [28].

The time required for a printable mortar to build-up its structure increases with SP content due to the reduction in attractive forces [29]. This can be overcome by using accelerators or VMA admixtures to increase the rigidification rate. Indeed, as shown in Fig. 11, the restructuration and re-flocculation rates increased with VMA concentration. On the other hand, the viscosity recovery rate R increased up to a certain limit. This suggests the existence of an optimum VMA dosage beyond which the recovery of the initial apparent viscosity is limited, which may deteriorate the printability of the mixture. The initial increase can be due to the thickening response of the long chains of VMA, while the lowest recovery rate can be due to the repulsive dispersion induced by SP. This behavior has been also reported in literature [17, 27].

Replacing fly ash with limestone fillers improved the re-flocculation rate. This is mainly due to the physico-chemical effect of limestone fillers, including better packing density and higher nucleation sites, as explained in the previous section. However, the replacement of silica fume by kaolinite promoted the granular stacking and, therefore, reduced the flocculation-induced restructuration rate of the mixture, but accelerated its rigidification by nucleation, reflected by higher G'_r values of LF-K and FA-K systems.

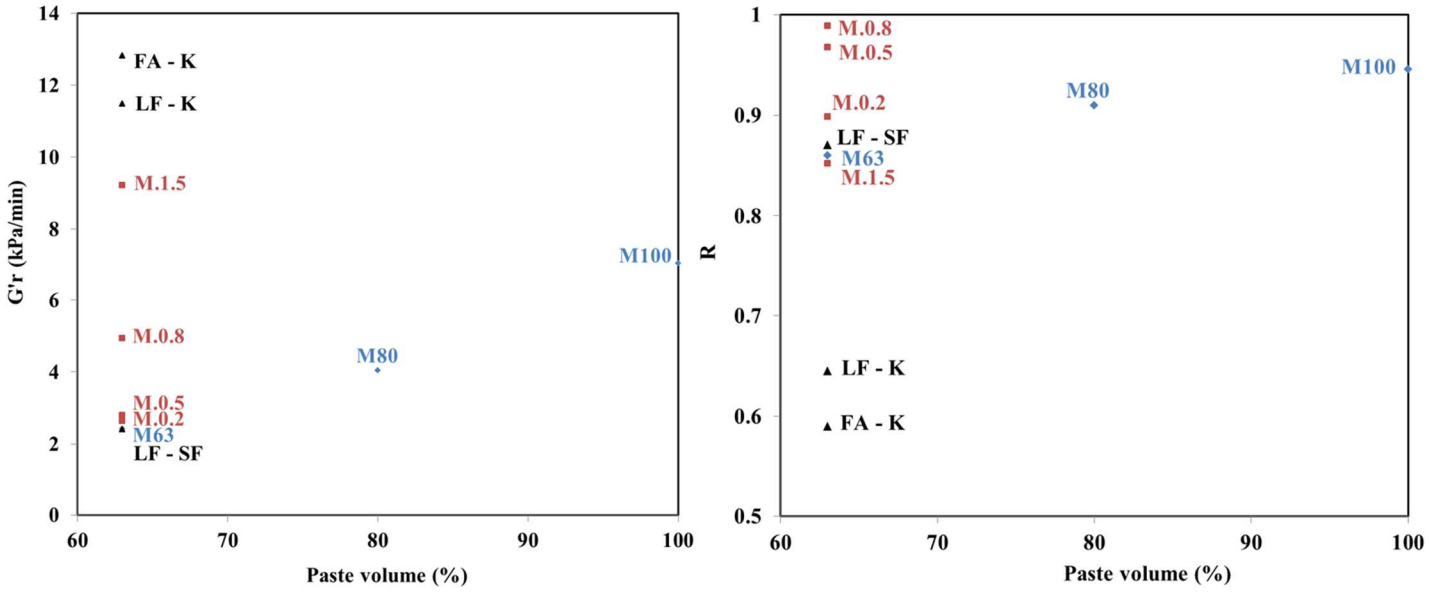

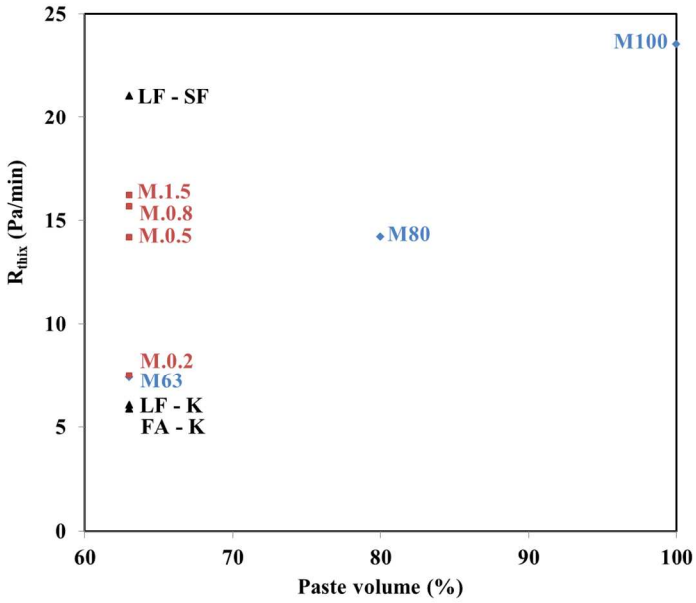

Fig. 11. Extrudability parameters of the investigated mixtures

At this stage, the determined parameters are relevant to assess the printability of the investigated mixtures, especially in the case of short-printing-period trials. Taken into consideration the time-dependent behavior of cement-based materials, monitoring their physico-chemical structuration may be necessary to assess the long-term evolution, which may not be possible to assess using the rheological parameters.

4.2 Buildability parameters of the mixtures

Results of the strain sweep measurements conducted on the investigated mixtures are shown in Fig. 12. On the other hand, the values of G' and critical strain are summarized in Table 4. As can be observed, the M100 mixture exhibited the highest storage modulus and critical strain compared to M80 and M63 mixtures. This can be due to cement particles interaction and higher packing density of the system. The presence of sand particles and SP can improve the dispersion state of cement particles, hence reducing attraction and increasing interparticle distances. The M100 mixture showed also a higher increase of G" before the drop compared to other mixtures. This may be related to its high apparent viscosity value due to denser microstructure and higher interparticle friction before flowing.

The addition of VMA up to 0.8%, by weight of cement, increased the storage modulus and critical strain to a certain limit. The use of higher dosage reduced the critical strain, hence reflecting the complex competition between SP and VMA due to their opposite effects.

The mixtures containing kaolinite exhibited a wider viscoelastic domain than those containing silica fume, hence reflecting better dispersion of the mixtures containing kaolinite. As mentioned earlier, this is due to the contribution of its particle-size distribution in improving the skeleton of the mixture. The LF-K and FA-K mixtures exhibited similar G" evolution than M100, which is consistent with high viscosity values. On the other hand, the incorporation of limestone filler resulted in lower critical strain compared to that observed with FA. This is mainly due to the dilution effect of LF, hence contributing in a smaller deformation needed to initiate the flow.

The open-time values of the investigated mixtures are shown in Table 5. In terms of the workability and extrudability parameters, it is expected that M63 mixture would exhibit longer open time compared to the other mixtures due to its relatively high SP dosage, which delayed the hydration reaction [28]. On the other hand, the induction period decreased with the VMA concentration up to 0.8%, by weight of cement. Beyond this dosage, the trend showed a turning point.

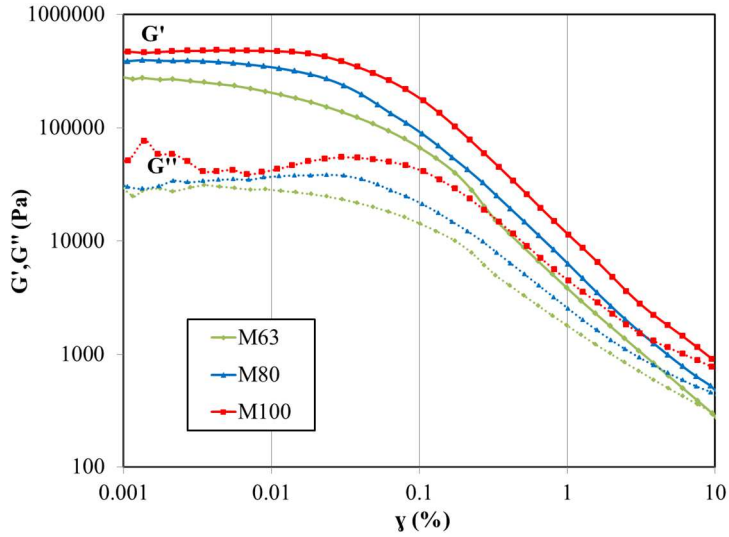

357

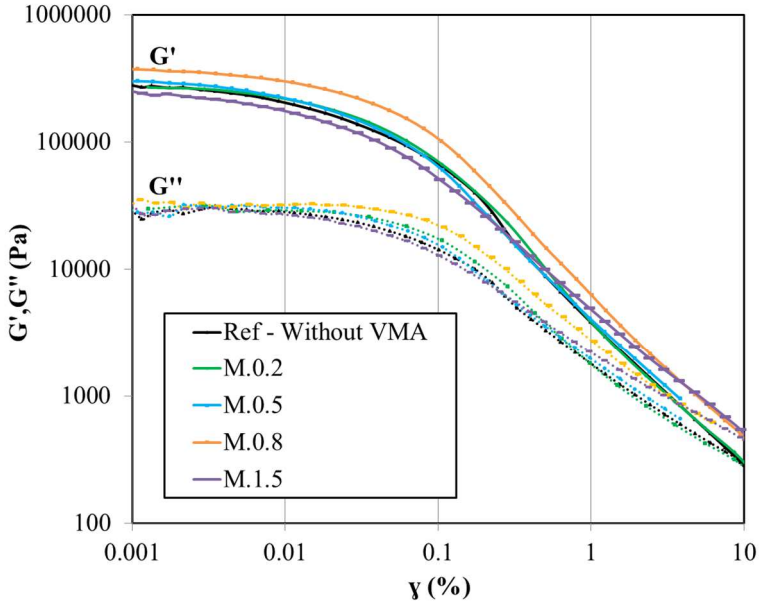

358

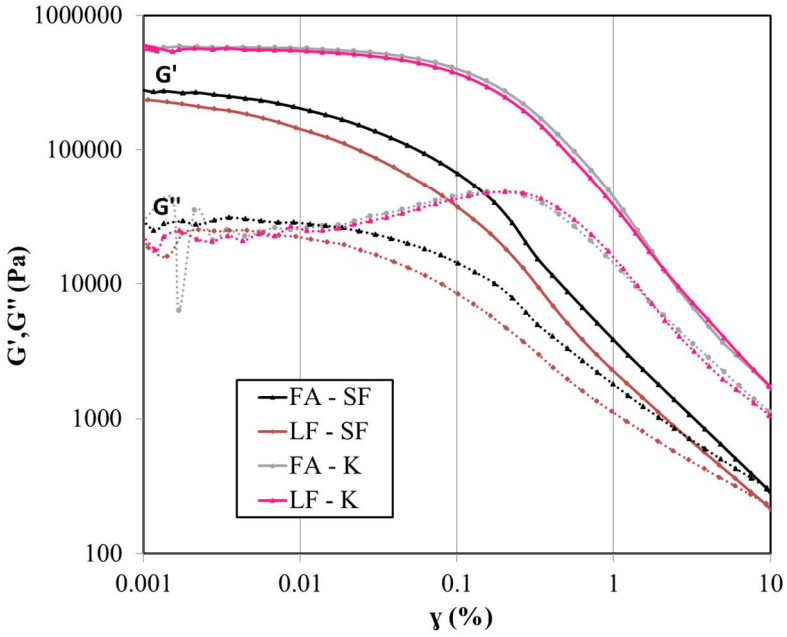

359

360 Fig. 12. Stain sweep results of the investigated mixtures

Table 4. The storage modulus and critical strain values of the investigated mixtures

	G' (10^5 Pa)	ɣc (10^{-1})
M100	4.51	17.7
M80	3.48	8.89
M63 (FA-SF)	2.51	3.52
M.0.2	2.47	4.86
M.0.5	2.52	5.64
M.0.8	3.05	8.95
M.1.5	2.1	4.47
FA - K	5.52	22.1
LF - SF	1.96	2.25
LF - K	5.15	17.5

Table 5. Open time values of the investigated mixtures

Mix	Open time (h)	
	Measured value	**Normalised Value**
M100	3.26	1.00
M80	6.00	1.84
M63	8.00	1.33
Ref - M63	8.00	1.00
M-0.2	5.50	0.69
M-0.5	5.00	0.63
M-0.8	4.22	0.53
M-1.5	6.50	0.81
FA-SF	8.00	1.00
FA-K	3.54	0.32
LF-SF	5.36	0.67
LF-K	2.56	0.44

As stated earlier, the competition between SP and VMA may be the origin of open-time variation. In fact, at low VMA concentration, the available long chains can adsorb onto cement particles without hindering the hydration kinetics [31]. In the case of higher dosage, only very few cementitious particles are exposed to water, which slow down the hydration. The adsorption of SP molecules can also contribute in delaying the hydration. In this context, the flow curves of (water – SP – VMA) system were compared with that of (water - VMA) combination for different dosages of VMA to evaluate the effect of admixtures on the mixing water flow behavior. As can be observed in Fig. 13, the viscosity of water is greatly affected by incorporating SP and VMA. On the other hand, the fluidification efficiency of SP is higher in the case of high VMA dosages mixtures. This reflects the SP-VMA interaction, which confirms what has been reported in literature [17], [32].

The incorporation of supplementary cementitious materials also affected the hydration kinetics. Indeed, the results presented in Table 5 revealed that replacing silica fume by kaolinite reduced by three times workability period (open time). This is mainly due to the relatively higher water demand of kaolinite compared to that of silica fume. This is consistent with the previous workability parameters. The accelerating effect of limestone fillers was also observed when it is combined with either silica fume or kaolinite. This may be attributable to its tri-fold effects, including (1) better packing density, (2) increased surface area per unit cement available for nucleation and growth of hydration products, and (3) the reactivity of the limestone fillers itself [31–33].

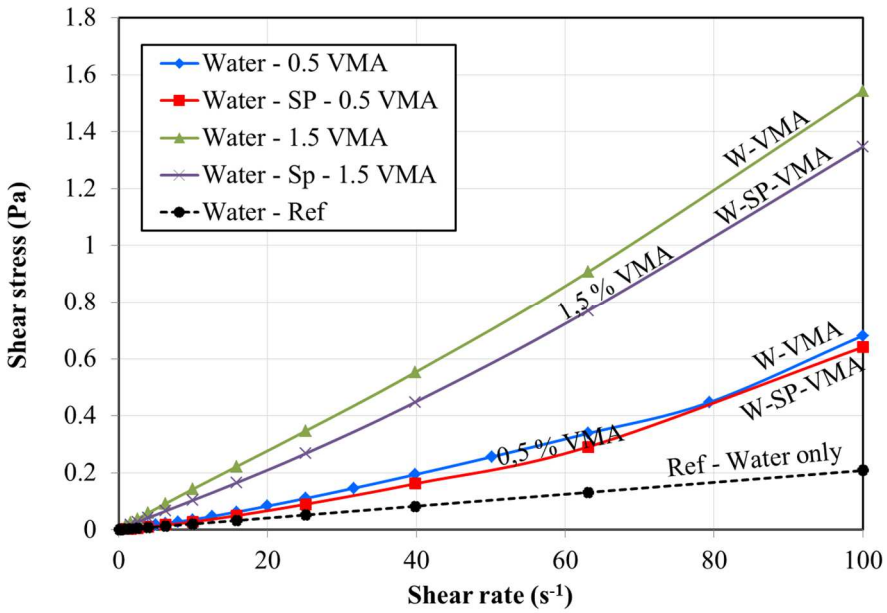

Fig. 13. Flow curves of water mixtures, with Sp and VMA at low and high dosages

In general, depending on the targeted printing time and strength development, adding VMA or combining different SCMs can be effective in achieving suitable parameters for successful printing process. The evolution of the elastic modulus with degree of hydration of the investigated mixtures is shown in Fig.14. The obtained results showed that the shear modulus followed the same trend of the Young modulus.

It is worthy to mention that the addition of VMA did not have a significant effect on the elastic modulus of the investigated mixtures. Indeed, its effect was limited at early-age during the induction period. On the other hand, combining different SCMs influenced the elastic behavior of the investigated mixtures at the hardened state. However, the strength development during the open-time was comparable, regardless of the type of SCMs. The mixture containing silica fume exhibited the highest elastic modulus at early age compared to other mixtures. This may be attributed to its higher reactivity compared to other SCM types. On the other hand, the accelerated hydration and improved early-age strength development observed with limestone fillers may be due to the stabilization of ettringite that increases the volume of hydration products, hence improving the compact-

ness and strength of the matrix [36]. These results suggest that the LF-SF mixture exhibited the best buildability aspect in terms of open time and strength, while M100 and M80 mixture showed the lowest constructability parameters.

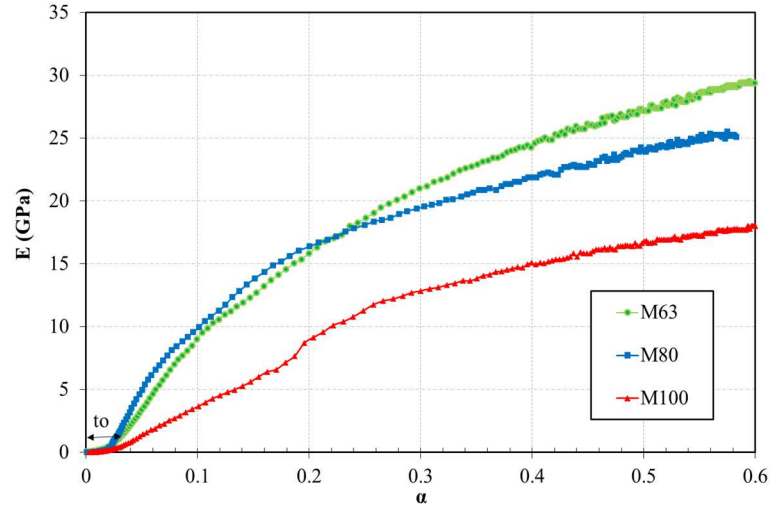

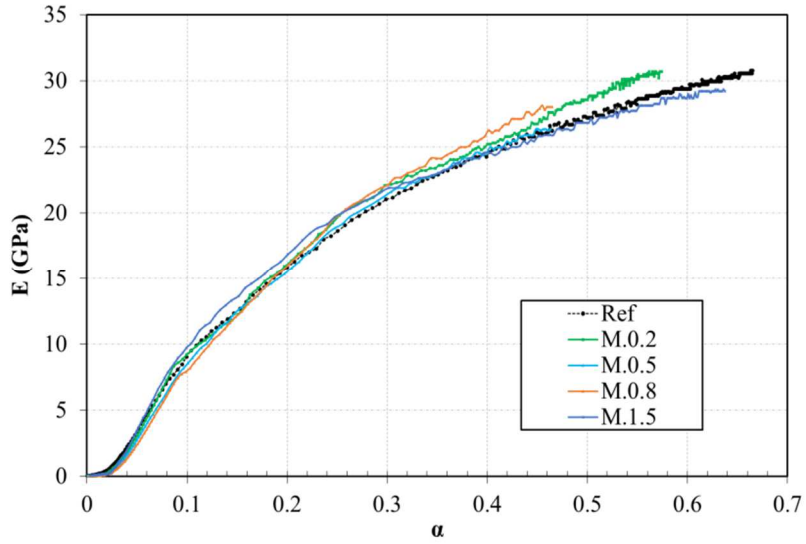

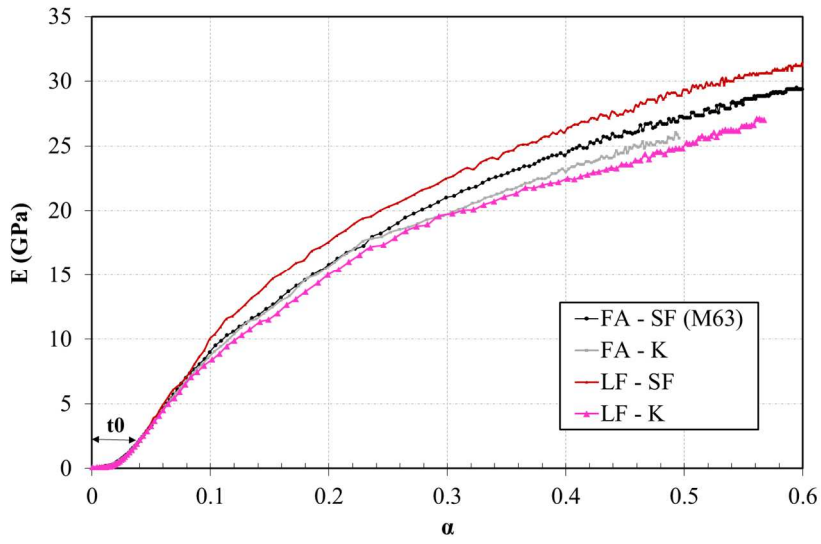

Fig. 14. Evolution of the elastic modulus with degree of hydration of the investigated mixtures

4.3 Printability validation

For comparison purposes, three indices reflecting workability, extrudability, and buildability aspects of the investigated mixtures, were defined, as follow:

$$W = \frac{\tau_{s0}}{\eta_{app}} , \qquad E = \frac{R_{thix}}{G'_r}.R , \qquad B = \frac{A_{thix}}{t_0}$$

where W, E, and B represent the workability, extrudability, and buildability indices, respectively. It is worth mentioning that these parameters are based on the previously identified parameters. Since the printing-time-period is short, the evolution of viscoelastic properties at latter age has not been taken into consideration in the buildability index. The determined parameters W, E, and B of the investigated mixtures are summarized in Fig.14. These printability WEB indices can be useful in facilitating the selection of optimum design to achieve successful printing quality, and predicting in advance the challenges that may occur during the printing process, as shown in Fig.1 (e.g. blockage, failure).

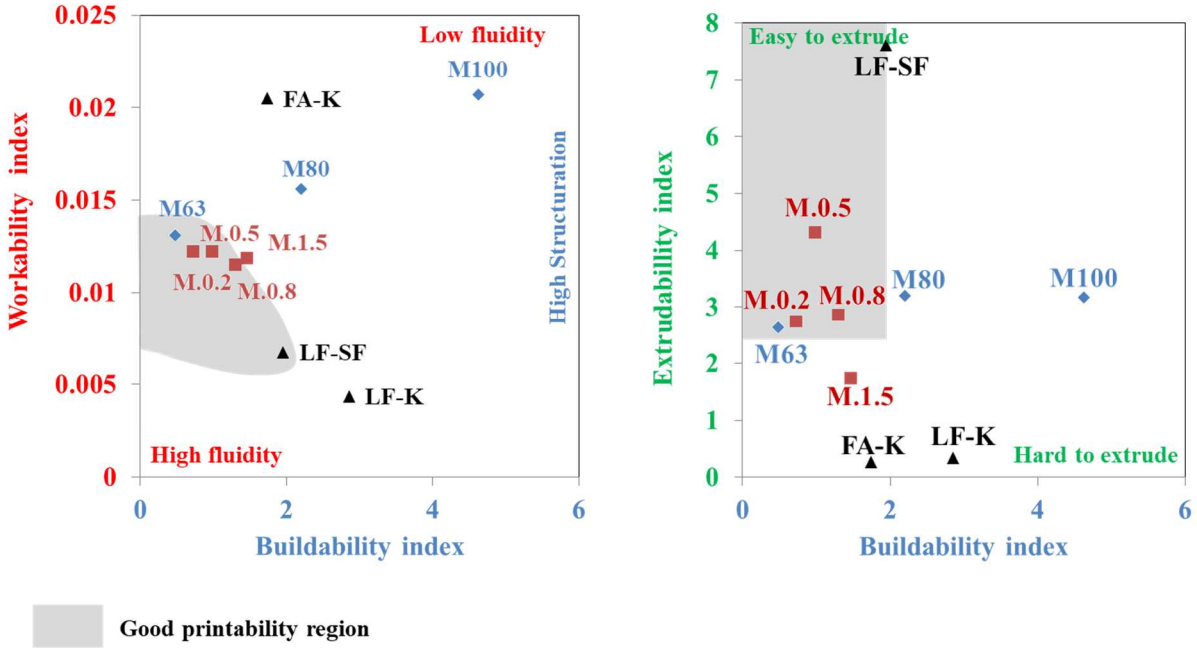

Fig. 15. W.E.B indices of the investigated mixtures

Various printing trials were conducted to validate the printability aspects of the investigated mixtures, as shown in Table 6. Based on the obtained results, it can be observed that mixtures with the lowest workability and extrudability and the highest buildability indices resulted in the lowest quality of filament surfaces. This was evaluated in terms of air voids, cracks, and deformations appearing during the printing process (M100, LF-K, FA-K, and M.1.5 mixtures). The M63 mixture showed very good extrusion quality and good interlayer adhesion, but moderate rate of constructability. However, the addition of VMA dosage less than 0.8%, by weight of cement, improved the rate of constructability. The use of higher dosage affected the quality of the extrusion, as observed with M.1.5 mixture. The extrudability index obtained with M.1.5 (E=1.7) is lower than that of M63 made

without any VMA (E =2.6). On the other hand, the LF-SF mixture exhibited very good buildability rate even with quite low viscosity and initial yield stress values. This can be due to its high rate of re-flocculation and structuration, thus increasing its extrusion ease and shape retention. A targeted W, E, and B corresponding to $0.006 < W < 0.015$, $E > 2.5$, and $B < 2$ (Fig. 14) can ensure good printability. Since a single batch approach was used for the printing, increasing the number of print layers resulted in decreasing the extrudability of mortar mixtures, especially those having high A_{thix} and G'_r, corresponding to mixtures with high values of E and B. This confirms the fact that the initial rheological properties are not sufficient to assess the printability of cement-based materials, hence the extrudability parameters are found to be more relevant in this regard. On the other hand, as expected the pumping pressure was found to increase with the apparent viscosity of the printed mixtures.

4.4 Recommendations

Based on the results discussed above, the following ~~useful~~ recommendations can be established to design printable cement-based materials for 3D printing:

- The trade-off between paste volume and SP content aims at facilitating the extrusion while taking into account the rate of constructability.
- The use of adequate VMA dosage (up to 0.8%, by weight of cement, in the case of this study) showed great potential in increasing the buildability cement mortars in 3D-printing, without affecting their strength development in the hardened state. However, higher dosage can deteriorate the extrusion quality. On the other hand, good compatibility between cement, SP, and VMA is essential to achieve adapted WEB parameters for successful printing.
- The effects of supplementary cementitious materials (SCMs), used as partial replacement of cement, on the open time and strength development depend on their type and content. For example, the combination of silica fume and limestone filler was shown to be favorable for 3D printing applications. On the other hand, the use of kaolinite has deteriorated both the workability and extrudability aspects of the investigated mixtures but improved the buildability rate. This can be due to the relatively high content (10%) used in this study.
- In addition to improve the printability aspects, the use of the SCMs reduces the carbon footprint of cement-based materials.

Conclusions

A new approach to design printable cement-based materials has been described in this paper. The printability was evaluated in terms of workability, extrudability, and buildability (WEB) aspects. The investigated mixtures were proportioned to cover wide ranges of rheological properties, by var-

ying paste volume, superplasticizer content, incorporating VMA or using different SCMs. Based on the results obtained in the present study, the following conclusions can be drawn:

- The printability of the investigated mixtures is successfully correlated to their rheological parameters, including apparent viscosity (η), and static yield stress (τ_{s0}) as well as its evolution rate (R_{thix}, A_{thix}). This reflects the importance of structure formed during the flocculation process for early-age 3D printing process.
- The initial rheological properties are not sufficient to adequately evaluate the printability of cement-based materials. Their combination with the restructuration parameters (R, G'_r) is important to follow up the changes that can occur during the printing process. The printability of the mixtures may require adjustments given the printing speed, flow rate, and the height of print layers.
- The selection of the mixture design approach depends on the printing time and the targeted strength. The use of VMA is shown to be efficient on improving the rate of constructability, while supplementary cementitious materials are effective in modifying strength development, open time, and microstructure. The combination of both approaches can help to improve the printability of cement-based materials.

489 **Table 6. Results of the printing validation of the investigated mixtures**

Printing trials	Mix	Average extrusion pressure (bar)	Texture of the filament	Average number of printed layers	Printability comments
	M100	0.7	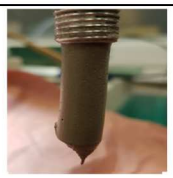	20	The filament is homogeneous. The buildability rate is high. The cohesion between the layers is not good enough considering the high rates of reflocculation and structuration comparing to the printing speed. The printability time is very limited, and air voids have been observed during the printing.
	M80	0.5		18	The extrusion quality is quite good. The bonding between the layers is fine. The constructability rate is close to that of the paste, and fewer air voids were seen on the filaments.
	M63	0.2	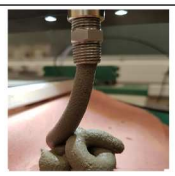	15	The mixture is very easy to extrude. Its fluidity allowed a better adhesion between the layers at a moderate rate of buildability. No air voids were noticed.
	M0.2	0.3		18	
	M0.5	0.5		23	By increasing the VMA dosage, the constructability rate increased due to the stabilising effect of the colloidal agent. On the other hand, the extrusion quality was deteriorated with the increase in VMA concentration. Microcracks and air voids reappeared on the surface of the filaments, particularly pronounced for M1.5. Sagging of some layers was also observed in M1.5 which reflects the heterogeneous nature of the mixture.
	M0.8	0.8	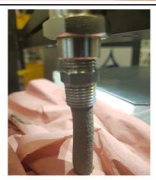	26	
	M1.5	1		25	
	LF - SF	0.5	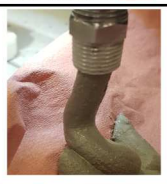	27	The mixture presents a good texture. Only slight deformation were observed. The printing time is large.
	LF - K	1.3		23	The geometry of the printed cylinder is very deficient. The texture of the filaments is heterogeneous but the shape stability is conserved.
	FA - K	1.5		23	The shape of the filament is perfect. The geometry is conserved but some layers show slight deformation. The printability time is restricted and the rate of buildability is high.

Acknowledgements

The financial support of the Ministry of Education of France is kindly acknowledged for the purchase of the 3D printer. The authors appreciate the technical support of the Civil and Mechanical Engineering Laboratory (GeM) and the Materials, Environment, Structures Department (MEO) of Centrale Nantes.

References

[1] H. October 2020, « Digitalisation how covid-19 is driving change in construction », *Building*. https://www.building.co.uk/sponsored-content/digitalisation-how-covid-19-is-driving-change-in-construction/5108588.article (consulté le 5 décembre 2020).

[2] J. G. Sanjayan et B. Nematollahi, « 3D Concrete Printing for Construction Applications », in *3D Concrete Printing Technology*, Elsevier, 2019, p. 1-11. doi: 10.1016/B978-0-12-815481-6.00001-4.

[3] F. Bos, R. Wolfs, Z. Ahmed, et T. Salet, « Additive manufacturing of concrete in construction: potentials and challenges of 3D concrete printing », *Virtual Phys. Prototyp.*, vol. 11, n° 3, p. 209-225, juill. 2016, doi: 10.1080/17452759.2016.1209867.

[4] P. Shakor, J. Renneberg, S. Nejadi, et G. Paul, « Optimisation of Different Concrete Mix Designs for 3D Printing by Utilising 6DOF Industrial Robot », juin 2017. doi: 10.22260/ISARC2017/0036.

[5] Y. Chen *et al.*, « Improving printability of limestone-calcined clay-based cementitious materials by using viscosity-modifying admixture », *Cem. Concr. Res.*, vol. 132, p. 106040, juin 2020, doi: 10.1016/j.cemconres.2020.106040.

[6] T. S. Rushing *et al.*, « Investigation of concrete mixtures for additive construction », *Rapid Prototyp. J.*, vol. 23, n° 1, p. 74-80, janv. 2017, doi: 10.1108/RPJ-09-2015-0124.

[7] N. Roussel, « Rheological requirements for printable concretes », *Cem. Concr. Res.*, vol. 112, p. 76-85, oct. 2018, doi: 10.1016/j.cemconres.2018.04.005.

[8] L. Reiter, T. Wangler, N. Roussel, et R. J. Flatt, « The role of early age structural build-up in digital fabrication with concrete », *Cem. Concr. Res.*, vol. 112, p. 86-95, oct. 2018, doi: 10.1016/j.cemconres.2018.05.011.

[9] A. Kazemian, X. Yuan, R. Meier, et B. Khoshnevis, « Chapter 2 - Performance-Based Testing of Portland Cement Concrete for Construction-Scale 3D Printing », in *3D Concrete Printing Technology*, J. G. Sanjayan, A. Nazari, et B. Nematollahi, Éd. Butterworth-Heinemann, 2019, p. 13-35. doi: 10.1016/B978-0-12-815481-6.00002-6.

[10] J. Kruger, S. Zeranka, et G. van Zijl, « An ab initio approach for thixotropy characterisation of (nanoparticle-infused) 3D printable concrete », *Constr. Build. Mater.*, vol. 224, p. 372-386, nov. 2019, doi: 10.1016/j.conbuildmat.2019.07.078.

[11] F. Sanchez, « Tools of the Future - Printing Cement-Based Materials in 3D ». Consulté le: 17 janvier 2022. [En ligne]. Disponible sur: https://onlinepubs.trb.org/onlinepubs/webinars/201117.pdf

[12] F. Lyu, D. Zhao, X. Hou, L. Sun, et Q. Zhang, « Overview of the Development of 3D-Printing Concrete: A Review », *Appl. Sci.*, vol. 11, n° 21, p. 9822, janv. 2021, doi: 10.3390/app11219822.

[13] « Agent de viscosité pour béton | Master Builders Solutions », *France*. https://www.master-builders-solutions.com/fr-fr/products/mastermatrix/mastermatrix-sdc-100 (consulté le 21 décembre 2020).

[14] A. Perrot, D. Rangeard, et A. Pierre, « Structural built-up of cement-based materials used for 3D-printing extrusion techniques », *Mater. Struct.*, vol. 49, n° 4, p. 1213-1220, avr. 2016, doi: 10.1617/s11527-015-0571-0.

* Corresponding author

[15] N. Roussel, G. Ovarlez, S. Garrault, et C. Brumaud, « The origins of thixotropy of fresh cement pastes », *Cem. Concr. Res.*, vol. 42, nº 1, p. 148-157, janv. 2012, doi: 10.1016/j.cemconres.2011.09.004.
[16] R. Cortas, E. Rozière, S. Staquet, A. Hamami, A. Loukili, et M.-P. Delplancke-Ogletree, « Effect of the water saturation of aggregates on the shrinkage induced cracking risk of concrete at early age », *Cem. Concr. Compos.*, vol. 50, p. 1-9, juill. 2014, doi: 10.1016/j.cemconcomp.2014.02.006.
[17] « Effect of Welan Gum-High-Range Water Reducer Combinations on Rheology of Cement Grout », *ACI Mater. J.*, vol. 94, nº 5, 1997, doi: 10.14359/321.
[18] H. Bessaies-Bey, R. Baumann, M. Schmitz, M. Radler, et N. Roussel, « Effect of polyacrylamide on rheology of fresh cement pastes », *Cem. Concr. Res.*, vol. 76, p. 98-106, oct. 2015, doi: 10.1016/j.cemconres.2015.05.012.
[19] M. Sonebi et A. Perrot, « Effect of mix proportions on rheology and permeability of cement grouts containing viscosity modifying admixture », *Constr. Build. Mater.*, vol. 212, p. 687-697, juill. 2019, doi: 10.1016/j.conbuildmat.2019.04.022.
[20] M. Benaicha, X. Roguiez, O. Jalbaud, Y. Burtschell, et A. H. Alaoui, « Influence of silica fume and viscosity modifying agent on the mechanical and rheological behavior of self compacting concrete », *Constr. Build. Mater.*, vol. 84, p. 103-110, juin 2015, doi: 10.1016/j.conbuildmat.2015.03.061.
[21] D. K. Panesar et R. Zhang, « Performance comparison of cement replacing materials in concrete: Limestone fillers and supplementary cementing materials – A review », *Constr. Build. Mater.*, vol. 251, p. 118866, août 2020, doi: 10.1016/j.conbuildmat.2020.118866.
[22] Y. Fan, S. Zhang, S. Kawashima, et S. P. Shah, « Influence of kaolinite clay on the chloride diffusion property of cement-based materials », *Cem. Concr. Compos.*, vol. 45, p. 117-124, janv. 2014, doi: 10.1016/j.cemconcomp.2013.09.021.
[23] Y. Zhang, Y. Zhang, W. She, L. Yang, G. Liu, et Y. Yang, « Rheological and harden properties of the high-thixotropy 3D printing concrete », *Constr. Build. Mater.*, vol. 201, p. 278-285, mars 2019, doi: 10.1016/j.conbuildmat.2018.12.061.
[24] D. P. Bentz, S. Z. Jones, I. R. Bentz, et M. A. Peltz, « Towards the formulation of robust and sustainable cementitious binders for 3-D additive construction by extrusion », *Constr. Build. Mater.*, vol. 175, p. 215-224, juin 2018, doi: 10.1016/j.conbuildmat.2018.04.167.
[25] O. A. Mendoza Reales, P. Duda, E. C. C. M. Silva, M. D. M. Paiva, et R. D. T. Filho, « Nanosilica particles as structural buildup agents for 3D printing with Portland cement pastes », *Constr. Build. Mater.*, vol. 219, p. 91-100, sept. 2019, doi: 10.1016/j.conbuildmat.2019.05.174.
[26] H. Jeong, S.-J. Han, S.-H. Choi, Y. Lee, S. Yi, et K. Kim, « Rheological Property Criteria for Buildable 3D Printing Concrete », *Materials*, vol. 12, nº 4, p. 657, févr. 2019, doi: 10.3390/ma12040657.
[27] J. T. Kolawole, R. Combrinck, et W. P. Boshoff, « Rheo-viscoelastic behaviour of fresh cement-based materials: Cement paste, mortar and concrete », *Constr. Build. Mater.*, vol. 248, p. 118667, juill. 2020, doi: 10.1016/j.conbuildmat.2020.118667.
[28] M. T. Souza, I. M. Ferreira, E. Guzi de Moraes, L. Senff, et A. P. Novaes de Oliveira, « 3D printed concrete for large-scale buildings: An overview of rheology, printing parameters, chemical admixtures, reinforcements, and economic and environmental prospects », *J. Build. Eng.*, vol. 32, p. 101833, nov. 2020, doi: 10.1016/j.jobe.2020.101833.
[29] D. Marchon, S. Kawashima, H. Bessaies-Bey, S. Mantellato, et S. Ng, « Hydration and rheology control of concrete for digital fabrication: Potential admixtures and cement chemistry », *Cem. Concr. Res.*, vol. 112, p. 96-110, oct. 2018, doi: 10.1016/j.cemconres.2018.05.014.
[30] R. Bouras, A. Kaci, et M. Chaouche, « Influence of viscosity modifying admixtures on the rheological behavior of cement and mortar pastes », *Korea-Aust. Rheol. J.*, vol. 24, nº 1, p. 35-44, mars 2012, doi: 10.1007/s13367-012-0004-3.
[31] Ó. H. Wallevik et I. Níelsson, *PRO 33: 3rd International RILEM Symposium on Self-Compacting Concrete*. RILEM Publications, 2003.

588 [32] T. H. Phan, M. Chaouche, et M. Moranville, « Influence of organic admixtures on the rheologi-
589 cal behaviour of cement pastes », *Cem. Concr. Res.*, vol. 36, n° 10, p. 1807-1813, oct. 2006, doi:
590 10.1016/j.cemconres.2006.05.028.
591 [33] L. R. Gurney, D. P. Bentz, T. Sato, et W. J. Weiss, « Reducing Set Retardation in High-Volume
592 Fly Ash Mixtures with the Use of Limestone: Iimproving Constructability for Sustainability »,
593 *Transp. Res. Rec. J. Transp. Res. Board*, vol. 2290, n° 1, p. 139-146, janv. 2012, doi:
594 10.3141/2290-18.
595 [34] M. Aqel et D. K. Panesar, « Hydration kinetics and compressive strength of steam-cured cement
596 pastes and mortars containing limestone filler », *Constr. Build. Mater.*, vol. 113, p. 359-368, juin
597 2016, doi: 10.1016/j.conbuildmat.2016.03.031.
598 [35] T. Oey, A. Kumar, J. W. Bullard, N. Neithalath, et G. Sant, « The Filler Effect: The Influence of
599 Filler Content and Surface Area on Cementitious Reaction Rates », *J. Am. Ceram. Soc.*, vol. 96,
600 n° 6, p. 1978-1990, 2013, doi: https://doi.org/10.1111/jace.12264.
601 [36] A. Schöler, B. Lothenbach, F. Winnefeld, M. B. Haha, M. Zajac, et H.-M. Ludwig, « Early hy-
602 dration of SCM-blended Portland cements: A pore solution and isothermal calorimetry study »,
603 *Cem. Concr. Res.*, vol. 93, p. 71-82, mars 2017, doi: 10.1016/j.cemconres.2016.11.013.
604